Role of surface charges in dc gas-discharge systems with high-ohmic electrodes

E. L. Gurevich,* A. W. Liehr, Sh. Amiranashvili, and H.-G. Purwins
Institut für Angewandte Physik, Corrensstrasse 2/4, D-48149 Münster, Germany
(Received 29 October 2003; published 31 March 2004)

Surface charge of the electrodes is investigated for planar dc gas-discharge systems. Both analytical estimates and experimental data show that such a charge plays an important role for the dc systems with a high-ohmic electrode. This is demonstrated by several experiments concerning discharge establishment and pattern formation phenomena. The surface charge has an inhibitory role, as it diminishes the electric field in the gas. Due to the low mobility of the surface charges, their distribution can be nonuniform giving rise to the observable filamentary structure of the discharge. It is also shown that the surface charge effect can be naturally incorporated in existing phenomenological models of the planar discharge. Thereby one can explain several observable phenomena, such as stability, multiplicity, and motion of the localized structures.

DOI: 10.1103/PhysRevE.69.036211 PACS number(s): 89.75.Kd, 52.80.Dy, 82.40.Ck

I. INTRODUCTION

Localized structures in nonlinear dissipative media and modeling of their spatiotemporal dynamics are of recent interest, since they lead to a growing number of possible or realized applications, e.g., data transmission on the basis of dispersion-managed solitons [1], the guidance of traffic and related self-driven many-particle systems [2,3], or parallel processors in the context of unconventional computing [4], which, for example, can be applied to the parallel estimation of Voronoi diagrams [5].

Experimentally self-organized localized structures, so-called dissipative solitons [6,7], are best observed in vertically oscillated granular media, hydrodynamical and optical systems, chemical media, and gas-discharge systems with a high-ohmic electrode [8–13]. While the modeling of chemical media commonly involves the identification of reacting species, formulating their reaction laws, and reducing the resulting set of equations, gas-discharge systems are either investigated on the basis of microscopic models [14,15], or phenomenologically on the basis of two-component reaction diffusion equations [16–19], where the activating component is related to the avalanche multiplication of charged carriers in the gap, while the voltage drop at the high-ohmic electrode plays the role of the inhibitor.

While two-component models comprehensively describe structure formation phenomena in one-dimensional dissipative systems, the situation is much more complicated in two-dimensional systems. Concerning current-driven planar gas-discharge systems with the high-ohmic electrode such qualitative activator-inhibitor models explain the existence of Turing patterns such as stripes or hexagonal patterns [20–23], spirals [24,25], stationary localized structures [19,26–28], and moving single dissipative solitons [29], but fail to explain the observation of several moving and interacting dissipative solitons [19,30,31], since the proposed stabilizing integral feedback does not take account of antisymmetric disturbances [32,33]. However, this problem can be easily overcome by introducing phenomenologically a second inhibiting component, which acts as a local feedback and stabilizes the dissipative solitons, such that the experimentally observed phenomena of scattering, formation of molecule-like bound states, or generation of dissipative solitons in many particle processes can be reproduced [31,33–35]. Furthermore, the phenomenological three-component reaction-diffusion system enables the description of the dynamics of dissipative solitons in terms of a particle ansatz [34], which has triggered the experimental detection of the theoretically predicted drift bifurcation of dissipative solitons and the measurement of the interaction law of dissipative solitons [29,36].

The obvious similarity of structure formation phenomena in planar gas-discharge systems and phenomenological three-component reaction-diffusion equations raises the question on the physical origin of the second inhibiting component. It should be of the same nature as the first inhibitor and should therefore be related to an additional voltage drop over the high-ohmic layer. The drop can be attributed to the surface charges accumulated on the electrodes. Moreover, the surface charge can be considered as a dynamical variable; the corresponding time scale should be equal to the Maxwell time τ_m. In this paper we investigate such a possibility both experimentally and analytically. The surface charges are well known to play a critical role in ac systems [37], with dielectric coating of the electrodes where τ_m is formally infinite. On the contrary, for DC systems with the high-conducting electrodes (e.g., $\tau_m \to 0$) the surface charge does not affect discharge properties. Our system is a mixed one, as the cathode is a high-ohmic electrode. The relatively large value of τ_m coexists here with the dc electric current. Our goal is to investigate the role of the surface charges in this situation.

We start with the simple estimates to show that considerable quantity of charge must be deposed on the electrodes. The induced electric field appears to be comparable with the Townsend (breakdown) electric field [38], that is, it significantly affects the discharge. Such an influence is then experimentally demonstrated. The surface charge is also shown to play an important role for transition between different states of patterned discharge. To conclude, we discuss our findings in the context of reaction-diffusion models [16,19,27]. We

*Corresponding author.
Email address: gurevich@uni-muenster.de

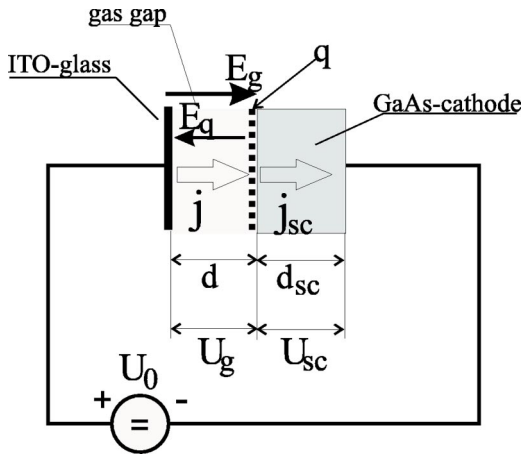

FIG. 1. Schematic representation of the dc planar gas-discharge cell.

demonstrate that the surface charges, being intrinsic for the high-ohmic electrode, act as the second inhibitor and provide an additional component for the considered activator-inhibitor system. The three-component reaction-diffusion model is finally justified to describe the dc gas discharge with the high-ohmic electrodes.

II. ESTIMATION OF THE SURFACE CHARGE

The planar semiconductor/gas-discharge cell is one of the systems, which is commonly used to investigate pattern formation in laboratory conditions. Its configuration is schematically shown in Fig. 1. The discharge cell is a three layer structure consisting of a gas-discharge gap edged from both sides with a low-ohmic anode and a high-ohmic cathode. After the external voltage U_0 is applied to the electrodes, the ignition takes place [19,22,23,25]. Increase in the voltage or in the discharge current causes a variety of transition scenarios between homogeneous and patterned forms of the discharge. The patterns result in nonuniform discharge luminance, the latter can be observed through the transparent electrode (normally through the low-ohmic anode).

In contrast to the dielectric-barrier gas discharge [37], the surface charge in the dc case does not require a separate consideration [38], as it instantly follows changes in the electric field. However, in the case of the high-ohmic electrode the Maxwell time (for semi-insulated GaAs $\tau_m = 10^{-4}$–10^{-6} s) is larger or comparable to the typical duration of discharge processes. The evolution equation for the surface charge comes therefore into play. Consequently, the ions deposited on the surface of the high-ohmic cathode are not neutralized immediately, but influence the discharge through their electric field. The electrical field E_q produced by the ions diminishes the external field in the gas. Let us consider the simplest Townsend mode of the discharge. The resulting field must then be equal to the Townsend field to maintain the self-sustained discharge [38].

It is now instructive to estimate the cathode surface charge for typical experimental conditions. Its density q causes the discontinuity of the electric field on the electrode surface, so that

$$\varepsilon E_{\mathrm{sc}} - E_g = \frac{q}{\varepsilon_0}, \tag{1}$$

where E_{sc} and E_g are the electric fields in the bulk of the semiconductor cathode and gas, respectively, ε being the cathode dielectric constant. For GaAs cathode used ins Refs. [19,25,30,39] and for Si cathode used in Ref. [40] $\varepsilon \approx 10$.

In the stationary case the surface charge density is constant, consequently the current densities in the gas and in the semiconductor are both equal to j, the latter is directly measured in experiments. The conductivity of the cathode σ for the GaAs wafers used in Refs. [19,25,30,39] was varied in the range from 0.1×10^{-7} $(\Omega\ \mathrm{cm})^{-1}$ to 3.0×10^{-7} $(\Omega\ \mathrm{cm})^{-1}$. In Ref. [40] the Si wafer has been additionally cooled to obtain the conductivity of the same order of magnitude. For given conductivity one calculates the electric field in the cathode simply through $E_{\mathrm{sc}} = j/\sigma$.

Substituting the E_{sc} into Eq. (1) one obtains the value of the surface charge density

$$q = \varepsilon_0 \left(\frac{\varepsilon j}{\sigma} - E_g \right), \tag{2}$$

as a function of the experimental control parameters.

The additional electric field E_q, which is produced by the surface charge and which diminishes the field in the gas gap, is to be estimated. The gap of the discussed experimental system is less than 1 mm although the diameter of the active gas-discharge area is of some centimeters. According to the big aspect ratio of the system we can consider our planar gas-discharge cell to be made of two infinitely large planes. Thus, the equation for the electric field produced by a charged infinite plane $E_q = q/(2\varepsilon_0)$ can be used.

To test if this charge density should be taken into account we compare E_q with the total electric field in the gas E_g. The latter is equal to the Townsend electric field E_T for the dark discharge or less than E_T for the glow discharge [38]. The value of E_q is seen to increase linearly with increase of j, that is, $E_q = E_T$ for some critical value $j = j_c$. It is straightforward to say that $j_c = 3\sigma E_T/\varepsilon$. For $\sigma = 0.2\times10^{-7}$ $(\Omega\ \mathrm{cm})^{-1}$, corresponding to the external illumination of the semiconductor electrode used in Ref. [36], one obtains $j_c = 30\ \mu\mathrm{A/cm}^2$. This value is much lower then the actual current density observed in the experiment. Similar analysis with the same result can be performed also for Refs. [30,40] and other experiments devoted to pattern formation phenomena in a dc gas-discharge cell with the high-ohmic electrode. That is, the electric field in the gas gap is, in fact, formed by surface charge accumulated on the high-ohmic layer.

Equation (2) can be plotted as a line in the plane of experimental control parameters (U_0, j). Both lines and the current-voltage characteristic of the discharge cell are schematically shown in Fig. 2 (the dashed and solid lines respectively). The characteristics are shown in a semilogarithmical scale, consequently the dashed line, being defined by the Eq. (2), looks like an exponential function. The dashed line divides the parameter space in two regions with $E_q < E_T$ and $E_q > E_T$. The critical discharge current j_c corresponds to the intersection point and is calculated from Eq. (2) with E_q

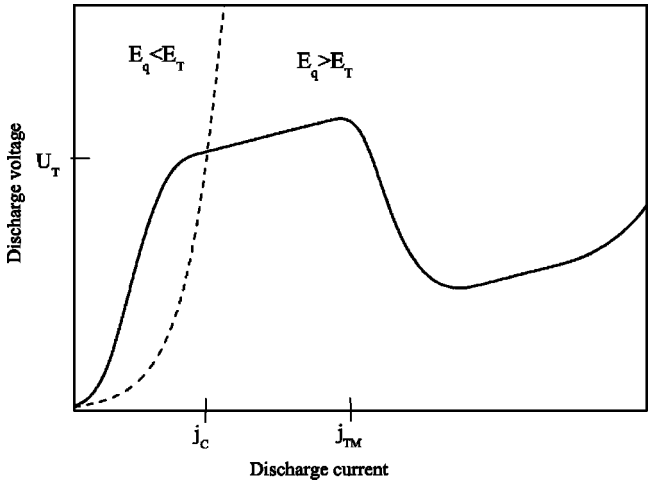

FIG. 2. The current-voltage characteristic of the discharge cell (solid line) is schematically shown in the semilogarithmic scale. The dashed line corresponds to the condition $E_q = E_T$ and is calculated according to Eq. (2) for GaAs electrode with $\sigma_{sc} = 0.2 \times 10^{-7}$ $(\Omega\ \mathrm{cm})^{-1}$, $\varepsilon_{sc} = 13$, $d = 0.15$ cm, $d_{sc} = 0.05$ cm, and $E_T = 6000$ V/cm, corresponding to discharge in nitrogen by the pressure $p = 35$ Torr

$= E_T$. It is found to be 30 μA/cm^2 for typical value $\sigma = 0.2 \times 10^{-7}$ $(\Omega\ \mathrm{cm})^{-1}$. On the other hand, the current density j_{TM} corresponding to the transition from the Townsend to the glow mode is $j_{\mathrm{TM}} \approx 850$ μA/cm^2 [38] for the conditions corresponding to Fig. 2. Experiments on pattern formation were also made with cooled Si cathode [19,40]. Conductivity of the Si wafer cooled down to 100–150 K is of the same order as above, thus our estimation is valid also in this case.

The estimations show that $j_{\mathrm{TM}} \gg j$. We stress that the pattern-formation phenomenon in the dc gas-discharge system occurs during the transition between the Townsend and the glow discharge (see, e.g., Refs. [19,30,36,39,40]). The surface charge must therefore play a significant role for the pattern formation. In particular, the cited experiments should be modelled with the three-component activator-inhibitor system presented in Refs. [33,41], but not with the two-component system presented in Ref. [16]. Also for Refs. [25,42] the surface charge should play an important role, though the patterns here were attributed to the nonlinear processes in the semiconductor cathode.

III. EXPERIMENTAL STUDY OF THE SURFACE CHARGE IN THE DISCHARGE SYSTEM

Experimental study of the surface charge in a dc gas-discharge system is very complicated, and to our knowledge, it has not been done yet. We present here a indirect proof that the charge on the surface of an high-ohmic electrode influences the discharge processes.

The experimental setup is a dc-driven planar gas-discharge system with a high-ohmic cathode similar to that, shown in Fig. 1. Diameter of the gas-discharge gap is 30 mm, its thickness d is 0.5 mm. The anode is transparent to visible light, which allows to observe the luminance distribution of the discharge. Semi-insulating GaAs wafer produced by the company ''Freiberger'' (Crystal 43725) is used as the cathode of the gas-discharge system. The thickness of the wafer d_{sc} is 1.5 ± 0.1 mm, its diameter is 50 mm. The conductivity of the semiconductor σ can be varied in experiments in the range from 0.1×10^{-7} $(\Omega\ \mathrm{cm})^{-1}$ to 3.0×10^{-7} $(\Omega\ \mathrm{cm})^{-1}$ due to the intrinsic photoeffect by changing the external illumination intensity. For a detailed description of the setup see Refs. [25,30].

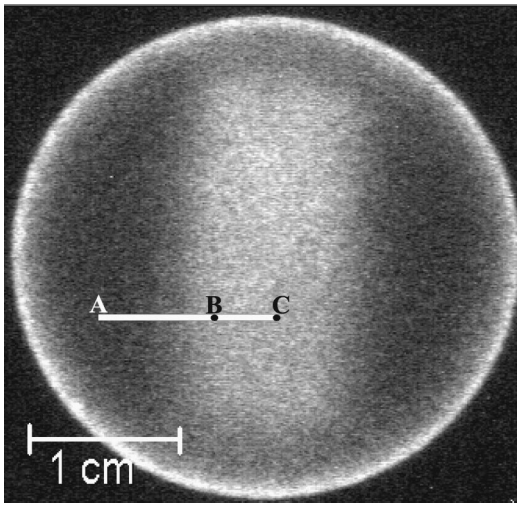

FIG. 3. Initial luminance distribution of the discharge in nitrogen by the pressure $p = 35$ Torr with partly illuminated GaAs cathode.

In the first phase of the experiment a small region of the semiconductor cathode (1 cm$\times$2 cm), which will be referred below as a ''central part'' of the gas-discharge area, has been illuminated through a mask. The rest of the cathode has not been illuminated at all. The illuminated area is 2 cm^2 while the active gas-discharge area is about 7 cm^2. The conductivity of the semiconductor cathode increases with the external illumination, thus the most of the discharge current flows through the illuminated area. The current distribution can be estimated through the discharge luminance distribution, which is shown in Fig. 3. According to Eq. (2) the charge on the illuminated cathode area is higher than that corresponding to the dark area.

In the second phase of the experiment we switch the external illumination off. As expected, the uniform distribution of the discharge luminance is established after some relaxation processes. The latter is rather nontrivial. The area, which was illuminated before, becomes *darker* as its surrounding. The dark spot slowly disappears and after approximately 2–3 s the discharge is uniform.

The dynamics of the gas discharge luminance profile along the line *AC*, which crosses the edge of the illuminated region, is shown in Fig. 4. The squares correspond to the first phase of the experiment. One can see that the luminance intensity of the central part is much stronger than that of the not illuminated area. This bright central part corresponds to the high current density, and consequently, to the high charge density on the surface of the semiconductor electrode.

After the external illumination has been switched off, one could expect a homogeneous distribution of the intrinsic lu-

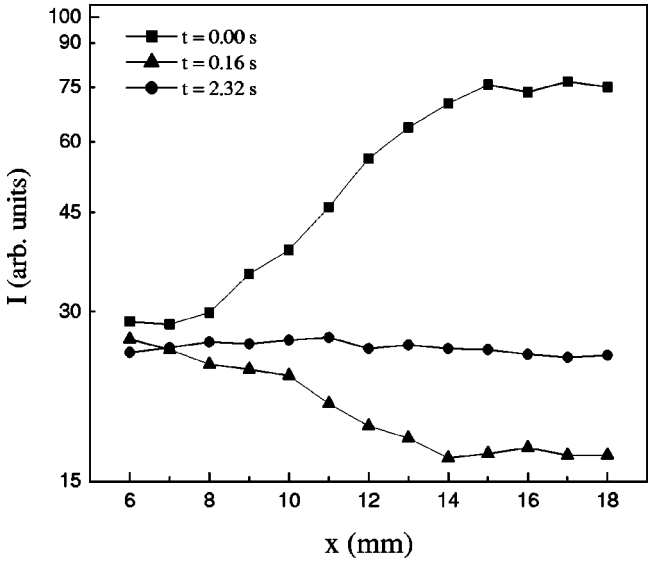

FIG. 4. The profiles of the edge of the luminance distribution along the line *AC* in Fig. 3 after switching off the external illumination. Intensity of the discharge luminance is presented in semilogarithmic scale in arbitrary units.

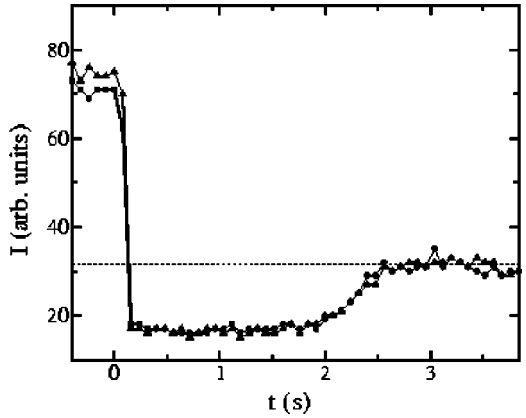

FIG. 5. The time dynamics of the luminance distribution shown in the points *B* (circles) and *C* (triangles) in Fig. 3 after switching off the external illumination. The dashed line corresponds to the average value of the background luminance.

minance, equal to the intrinsic luminance corresponding to the unilluminated area. But we observe in the second phase, that the intensity of the radiated light is lower in the central part of the discharge compared to the area, which has not been illuminated. It is shown by triangles in Fig. 4, demonstrating the light intensity distribution for $t=0.16$ s after the external light is switched off. That means that the discharge current density in the central part is now lower than the so-called dark current (i.e., the current in the area, which has not been illuminated). Although the resistivity of the semiconductor and the supply voltage are in the second phase uniform, the luminance profile becomes uniform only in about 2 s (see circles in Fig. 4). We note that the luminance of the unilluminated area conserves during the experiment.

This few-second delay, in which the discharge luminance is restored, does not reflect the real time scale of the surface charge, which is obviously much smaller. In reality the charge disappears from the cathode in less than one millisecond, and the next breakdown takes place not immediately, but after some delay [43,44]. The delay time of some seconds observed in the present experiment agrees with the experimental results obtained in Refs. [43,44].

The reduction of the discharge luminance under the background level can be explained if one takes into account the charge deposited on the surface of the high-ohmic electrode during the first phase of the experiment. This deposition takes place mostly in the area, where the discharge current density is higher, i.e., in the central part. After the external illumination has been switched off, the conductivity of the central part decreases, thus the Maxwell time of this part increases. Consequently, the surface charge then goes out of the equilibrium, because the source of the deposited charged particles is the same, but the sink is reduced. This process results in a local increase of the surface charge, which diminishes the local electric field in that central part of the gas-discharge gap. Charge carriers multiplication processes in gas discharge are very senstive to electric field [38], because the ionization coefficient depends on the field in the gap exponentially. That is why the current density (consequently, luminance of the discharge) in the central part is lower in the second phase of the experiment.

Other physical processes, but the surface charge storage, cannot clarify the observed phenomenon, because they would lead, in opposite, to the increase of the discharge luminance above the background level. The temperature gradient (if any) would increase the luminance of the central part of the discharge in the second phase of the experiment, because the conductivity of semiconductors increases with temperature. The excited atoms ease the ignition too. So, we interpret this effect as an experimental confirmation of the important role, which the charge deposited on the high-ohmic electrodes plays in gas-discharge processes.

The time evolution of the discharge luminance measured in points marked as *B* and *C* in Fig. 3 is shown in Fig. 5. One can see that starting from $t=0$ (at $t=0$ the external illumination has been switched off), the intensity of the externally illuminated region does not decrease monotonically. It decreases under the background level, which is shown in Fig. 5 as dashed line, and then restores to it in a couple of seconds. One can also see, that there is no difference in the luminance dynamics in points *B* (edge of the illuminated part) and *C* (center of the illuminated part). Consequently, no diffusion in lateral direction can be registered.

But the upper limit for the diffusion coefficient of nitrogen ions on the GaAs surface D_q can be estimated from the observed experimental data. The discharge luminance under the the background level has been measured in two points (*B* and *C* in Fig. 3) extending on $\Delta l=4$ mm from each other. The observation time $\Delta t \approx 2.5$ s, in which one cannot see the difference between the dynamics in these points (see Fig. 5). Consequently, the diffusion coefficient D_q is lower than the minimal diffusion coefficient we can estimate, i.e., $D_q < (\Delta l)^2/\Delta t \approx 0.06$ cm^2/s.

Such a low diffusion coefficient cannot be related to any of gas species, by which the diffusion coefficient is D_e

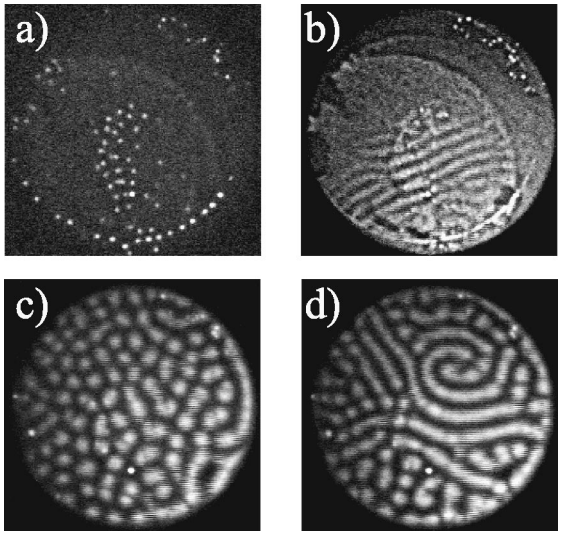

FIG. 6. Pattern in the nitrogen gas discharge by $p=110$ Torr, $T=110$ K, $d=0.05$ cm. Diameter of the gas discharge area $D=1.5$ cm. Semiconductor: Si⟨Pt⟩, thickness $a=0.12$ cm. (a) $U_0=1500$ V, discharge current $I=35$ μA; (b) $U_0=2200$ V, $I=148$ μA; (c) $U_0=1500$ V, $I=195$ μA; (d) $U_0=1510$ V, $I=238$ μA.

$\approx 10^4$ cm^2/s for electrons or $D_i \approx 1.5$ cm^2/s for ions [38,45] in gas discharge. This estimation is very important, because in Ref. [19] authors develop a semi-phenomenological reaction-diffusion model for pattern formation in a dc gas-discharge cell with high-ohmic semiconductor electrodes. The authors obtain pattern formation with the diffusion coefficients of the charge carriers $D_N=0.045$ cm^2/s, which is much lower than any of the diffusion coefficients of gas species, but fits the estimations for D_q. This example stresses ones again, that the charge on the surface of the high-ohmic electrode plays a significant role for pattern formation model development.

IV. THE SURFACE CHARGE AS A CONTROL PARAMETER FOR PATTERN FORMATION PHENOMENA

The role of the surface charge for pattern formation phenomena can be illustrated as follows. The gas-discharge cell shown in Fig. 1 was used for experimental study of large variety of pattern formation phenomena. The structures as stripes and current filaments are common in the discharge with high-ohmic silicon electrode by cryogenic temperatures [22,23]. Here we study the transition between these two patterns, as shown in Fig. 6, where the observations in the gas discharge with a Si⟨Pt⟩ (silicon doped with platinum) high-ohmic electrode are presented.

By low conductivity of the semiconductor the discharge ignites in the filamentary mode Fig. 6 (a). Increase in the cell voltage causes both motion of filaments and appearance of a moving Turing pattern, see Fig. 6 (b). By higher conductivities of the semiconductor wafer the bifurcation scenario is the same, but the structures are brighter and the transition between the filamentary mode and the Turing pattern occurs by lower voltage, see Figs. 6 (c) and 6(d). The corresponding bifurcation diagram in coordinates (U_0, σ) is shown in Fig. 7(a), where the transition between the filaments and stripes are shown for different temperatures. The curves divide the parameter space into two parts: the low values of U_0 and σ correspond to the filamentary mode of the discharge, the high values of U_0 and σ correspond to the stripes.

In this bifurcation diagrams the curves dividing the filamentary and the stripe modes in the parameter space are shown for different temperatures of the gas-discharge cell. If we calculate the total charge on the surface of the semiconductor q, we can plot the bifurcation diagram in new coordinates (U_0, q), see Fig. 7(b). Note that the several curves for different temperatures are actually replaced with only one curve. In other words, the value of the surface charge, by which the transition takes place, does not depend on temperature in contrast with conductivity, which is commonly used as a control parameter for pattern formation in a gas-discharge cell with high-ohmic electrodes. It is natural to assume that the considerations taking the surface charge on the high-ohmic layer into account can reveal the physical background of the pattern formation in gas-discharge systems with high-ohmic electrodes.

V. PHENOMENOLOGICAL MODEL

As it has been shown, the surface charge influences the physical processes in a gas-discharge system with a high-ohmic electrode. It should be therefore taken into account by elaborating an appropriate model. Detailed investigation of such an elaboration for classical discharge models is out of

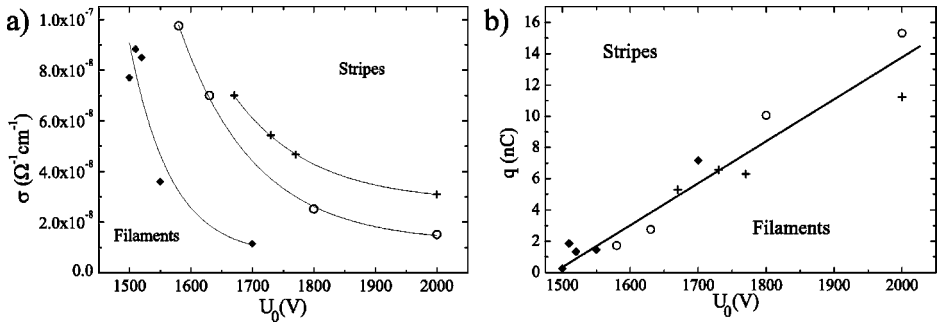

FIG. 7. The bifurcation diagram corresponding to the transition from filaments to stripes for different temperatures. ◆, $T=110$ K; ○, $T=133$ K; +, $T=143$ K. Diameter of the gas discharge area $D=1.5$ cm. Semiconductor: Si⟨Pt⟩, thickness $a=0.12$ cm. (a) In coordinates (U_0, σ), (b) in coordinates (U_0, q).

scope of the present paper. Here we restrict ourselves to a simple phenomenological model [16], which provides at least good qualitative understanding of pattern formation phenomena in our experimental system. In the cited paper an equivalent circuit has been used to derive a two-component reaction-diffusion system

$$u_t = D_u \Delta u + \lambda u - u^3 - \kappa_w w + \kappa_1,$$

$$\theta w_t = D_w \Delta w + u - w, \tag{3}$$

where the activator u and inhibitor w were interpreted as the current density and voltage drop over the high-ohmic electrode, respectively.

The two-component reaction-diffusion system (3) was later formally generalized to a three component one ([31,33–35]). The goal of this section is to demonstrate that the surface charge can be considered as a second inhibitor for such a system.

First, the surface charge was shown to diminish (i.e., to inhibit) the discharge current. The latter on the other hand produces (i.e., activates) the surface charge by depositing the charge carriers on the surface of the high-ohmic electrode.

The system (3) should then be completed with one more equation describing the dynamics of the surface charge q,

$$\dot{q} = D_q \triangle q + j - \frac{q}{\tau_m}, \tag{4}$$

where the electric current in the gas j increases q and the electric current in the semiconductor, being described through the Maxwell time τ_m, decreases q. The motion of the surface charges is described through the diffusion term, whereas the term connected with the surface curvature (see, e.g., Ref. [46]) can be ignored. The relation of Eq. (4) to the equations in the system (3) should be analyzed. The inhibitory role of the surface charge, as it diminishes the current density u, can be expressed by introducing a corresponding term (i.e., $-\kappa_3 v$ with $\kappa_3 > 0$) in the first equation of the system (3). After some renormalization we obtain the three-component reaction-diffusion system used formally in Refs. [33,41] without explanation of physical background of the third component.

VI. CONCLUSION

The role of the surface charge accumulated on the dielectric coating of the electrodes has been broadly discussed [37,38,47,48] for the ac gas-discharge systems. In the case of the dc gas discharge with high-conductive electrodes the extrinsic charges can be quickly removed from the electrodes and do not affect the discharge dynamics. That is why only the charging processes on the confining surfaces (e.g., dielectric walls and spacers) have been discussed in literature [38,43,49,50] for a dc discharge.

Conducting properties of semi-insulating semiconductors are between those of conductors and insulators. Consequently, one should raise the question whether the accumulated surface charge affects the discharge processes. The estimations claim that the influence of the surface charge on the gas discharge should be taken into account. The charge deposited on the electrodes inhibits the discharge in the system. It introduces an important time scale and produces the additional electric field in the gas gap, which is comparable with the Townsend electric field E_T [38] or exceeds it.

The mechanism of the inhibition can be summarized as follows: The charge carriers, being produced via ionization, are deposited on the electrodes. The extrinsic surface charge immediately vanishes on the low-ohmic electrode (e.g., on a metal plate), but on the surface of a high-ohmic electrode this process is delayed because of high resistivity (i.e., relatively large Maxwell time) of the latter. The charge is deposited and stored on the surface diminishing thus the external electric field. Then it results in the reduction of the discharge current. The temporal changes in the current cause changes in the surface charge, and the changes follow with some delay giving rise to nontrivial temporal dynamics. A similar mechanism can also be responsible for homogeneous oscillations of the discharge current as was found experimentally in Ref. [39].

Our experimental investigations also confirm that the surface charge diminishes the discharge current and acts as inhibitor. The experiment presents also a new method to study the charge dynamics on high-ohmic surfaces in a gas discharge.

ACKNOWLEDGMENTS

We thank the Deutsche Forschungsgemeinschaft (DFG) and the President of Grant of Russia for Scientific Schools Grant (Grant No. SS-2223.2003.2) for their support.

[1] J. Martensson and A. Berntson, IEEE Photonics Technol. Lett. **13**, 666 (2001).
[2] D. Helbing and T. Vicsek, New J. Phys. **1**, 13 (1999).
[3] D. Helbing, Rev. Mod. Phys. **73**, 1067 (2001).
[4] A. Adamatzky, in *Collision-Based Computing*, edited by A. Adamatzky (Springer, New York, 2002), pp. 411–442.
[5] A.L. Zanin, A.W. Liehr, A.S. Moskalenko, and H.-G. Purwins, Appl. Phys. Lett. **81**, 3338 (2002).
[6] M. Bode and H.-G. Purwins, Physica D **86**, 53 (1995).
[7] C.I. Christov and M.G. Velarde, Physica D **86**, 323 (1995).
[8] G. H. Ristow, *Pattern Formation in Granular Materials* (Springer, Berlin, 1995).
[9] A. V. Getling, *Rayleigh-Bénard Convection. Structure and Dynamics* (World Scientific, Singapore, 1998).
[10] F.T. Arecchi, S. Boccaletti, and P. Ramazza, Phys. Rep. **318**, 1 (1999).
[11] A. de Wit, Adv. Chem. Phys. **109**, 435 (1999).
[12] G. Ertl, Adv. Catal. **45**, 1 (2000).

[13] H.-G. Purwins, Y. Astrov, and I. Brauer, in *The Fifth Experimental Chaos Conference, Orlando, Florida, USA, 1999*, edited by M. Ding, W. L. Ditto, L. M. Pecora, and M. L. Spano (World Scientific, Singapore, 2001), pp. 3–13.
[14] I. Brauer, C. Punset, H.-G. Purwins, and J.P. Boeuf, J. Appl. Phys. **85**, 7569 (1999).
[15] R.S. Islamov, Phys. Rev. E **64**, 046405 (2001).
[16] H.-G. Purwins, C. Radehaus, and J. Berkemeier, Z. Naturforsch. A 17 (1988).
[17] C. Radehaus, H. Willebrand, R. Dohmen, F.-J. Niedernostheide, G. Bengel, and H.-G. Purwins, Phys. Rev. A **45**, 2546 (1992).
[18] B. S. Kerner and V. V. Osipov, *Autosolitons: A New Approach to Problems of Self-Organization and Turbulence*, Fundamental Theories of Physics Vol. 61 (Kluwer Academic, Dordrecht, 1994).
[19] Y.A. Astrov and Y.A. Logvin, Phys. Rev. Lett. **79**, 2983 (1997).
[20] A.M. Turing, Philos. Trans. R. Soc. London, Ser. B **237**, 37 (1952).
[21] M. Or-Guil, E. Ammelt, F.-J. Niedernostheide, and H.-G. Purwins, in *Pitman Research Notes in Mathematics Series*, edited by A. Doelman and A. van Harten (Longman, Harlow, 1995), Vol. 335, pp. 223–237.
[22] Y. Astrov, E. Ammelt, S. Teperick, and H.-G. Purwins, Phys. Lett. A **211**, 184 (1996).
[23] E. Ammelt, Y.A. Astrov, and H.-G. Purwins, Phys. Rev. E **58**, 7109 (1998).
[24] A. S. Mikhailov, *Foundations of Synergetics I. Distributed Active Systems*, Springer Series in Synergetics Vol. 51 (Springer, Berlin, 1990).
[25] E.L. Gurevich, A.S. Moskalenko, A.L. Zanin, Y.A. Astrov, and H.-G. Purwins, Phys. Lett. A **307**, 299 (2003).
[26] T. Ohta, M. Mimura, and R. Kobayashi, Physica D **34**, 115 (1989).
[27] C.P. Schenk, P. Schütz, M. Bode, and H.-G. Purwins, Phys. Rev. E **57**, 6480 (1998).
[28] S. Nasuno, Chaos **13**, 1010 (2003).
[29] A.W. Liehr, H.U. Bödeker, M.C. Röttger, T. Frank, R. Friedrich, and H.-G. Purwins, New J. Phys. **5**, 89 (2003).
[30] Y.A. Astrov and H.-G. Purwins, Phys. Lett. A **283**, 349 (2001).
[31] A. W. Liehr, A. S. Moskalenko, Y. A. Astrov, M. Bode, and H.-G. Purwins, Eur. J. Phys. B (to be published).
[32] K. Krischer and A. Mikhailov, Phys. Rev. Lett. **73**, 3165 (1994).
[33] C.P. Schenk, M. Or-Guil, M. Bode, and H.-G. Purwins, Phys. Rev. Lett. **78**, 3781 (1997).
[34] M. Bode, A.W. Liehr, C.P. Schenk, and H.-G. Purwins, Physica D **161**, 45 (2002).
[35] A. W. Liehr, A. S. Moskalenko, M. C. Röttger, J. Berkemeier, and H.-G. Purwins, in *High Performance Computing in Science and Engineering '02. Transactions of the High Performance Computing Center Stuttgart (HLRS) 2002*, edited by E. Krause and W. Jäger (Springer, Berlin, 2003), pp. 48–61.
[36] H. U Bodeker, M.C. Röttger, A.W. Liehr, T.D. Frank, R. Friedrich, and H.-G. Purwins, Phys. Rev. E **67**, 056220 (2003).
[37] W. Breazeal, K.M. Flynn, and E.G. Gwinn, Phys. Rev. E **52**, 1503 (1995).
[38] Y. P. Raizer, *Gas Discharge Physics*, 2nd ed. (Springer, Berlin, 1997).
[39] C. Strümpel, Y.A. Astrov, and H.-G. Purwins, Phys. Rev. E **62**, 4889 (2000).
[40] Yu.A. Astrov, I. Müller, E. Ammelt, and H.-G. Purwins, Phys. Rev. Lett. **80**, 5341 (1998).
[41] R. Woesler, P. Schütz, M. Bode, M. Or-Guil, and H.-G. Purwins, Physica D **91**, 376 (1996).
[42] Y.A. Astrov and H.-G. Purwins, Tech. Phys. Lett. **28**, 910 (2002).
[43] Z.L. Petrović, V.L. Marković, M.M. Pejović, and S.R. Gocić, J. Phys. D **34**, 1756 (2001).
[44] M.M. Pejović, G.S. Ristić, and J.P. Karamarković, J. Phys. D **35**, R91 (2002).
[45] I. S. Grigoriev and E. Z. Meilikhov, *Handbook of Physical Quantities* (CRC Press, New York, 1997).
[46] S. Amiranashvili, M.Y. Yu, L. Stenflo, G. Brodin, and M. Servin, Phys. Rev. E **66**, 046403 (2002).
[47] H. Kitabayashi, H. Fujii, and T. Ooishi, Jpn. J. Appl. Phys. **38**, 2964 (1999).
[48] H.S. Jeong, B.-J. Shin, and K.-W. Whang, IEEE Trans. Plasma Sci. **27**, 171 (1999).
[49] T. Jing, IEEE Trans. Dielectr. Electr. Insul. **2**, 771 (1995).
[50] F. Messerer, M. Finkel, and W. Boeck, in Proceedings of the IEEE International Symposium EI, Boston, 2002 (unpublished), pp. 421–425.